Available online at www.sciencedirect.com

SCIENCE DIRECT

European Journal of Pharmacology 505 (2004) 37–50

www.elsevier.com/locate/ejphar

Methoctramine analogues inhibit responses to capsaicin and protons in rat dorsal root ganglion neurons

Ian R. Mellor[a,*], Jane Ogilvie[b], Florentina Pluteanu[a,1], Richard H. Clothier[b], Terence L. Parker[b], Michela Rosini[c], Anna Minarini[c], Vincenzo Tumiatti[c], Carlo Melchiorre[c]

[a]School of Biology, University of Nottingham, University Park, Nottingham, NG7 2RD, UK
[b]School of Biomedical Sciences, University of Nottingham Medical School, Queens Medical Centre, Nottingham, NG7 2UH, UK
[c]Department of Pharmaceutical Sciences, University of Bologna, Via Belmeloro 6, 40126 Bologna, Italy

Received 24 June 2004; received in revised form 30 September 2004; accepted 4 October 2004
Available online 5 November 2004

Abstract

We have investigated the possibility that vanilloid receptors have a binding site for polyamines and determined the consequences of binding to such a site. Whole-cell and single-channel patch-clamp recordings were used to investigate the effect of the tetraamine, methoctramine, and 16 of its analogues on capsaicin and proton induced responses of foetal rat dorsal root ganglion neurons. All but two methoctramine analogues inhibited responses to 10 μM capsaicin with IC_{50} values in the range of 2–70 μM at a holding potential of –100 mV. Inhibition was generally non-competitive and voltage-dependent. Methoctramine at 10 μM reduced the single channel mean open time (>3-fold), but also increased the mean closed time (1.7-fold). Sustained responses to pH 5.4 were antagonized by methoctramine with similar potency to capsaicin responses. Similar data were obtained with adult rat dorsal root ganglion neurons. These data indicate that methoctramine analogues bind to vanilloid receptors to inhibit their function.

Keywords: Vanilloid receptor; Methoctramine; Channel block; Dorsal root ganglion; Patch-clamp; Polyamine

1. Introduction

Vanilloid receptor 1 (VR1) is a non-selective cation channel that can be activated by several stimuli including noxious heat, protons and vanilloid agonists (reviewed by Gunthorpe et al., 2002; Caterina and Julius, 2001; Szallasi and Di Marzo, 2000; Kress and Zeilhofer, 1999). The classical vanilloid agonist is capsaicin, the component of chilli peppers causing the 'hot' sensation. Cloning of VR1 (Caterina et al., 1997) showed it to be closely related to the transient receptor potential (TRP) family of ion channels. Hence, VR1 is now termed TRPV1 (Montell et al., 2002). TRPV1 is the only member of this family that can be activated by capsaicin and related vanilloids, however, heat activation is also known for TRPV2 (formerly VRL-1) and probably accounts for heat sensitive dorsal root ganglion neurons that are insensitive to capsaicin (Nagy and Rang, 1999; Savidge et al., 2001), while "warm"-activation is known for TRPV3 and TRPV4 (Benham et al., 2003). Recombinant homomeric TRPV1 are sensitive to both heat and capsaicin (Savidge et al., 2001). TRPV1 is also activated by protons and although it is the only TRP channel activated by low pH, other acid sensing ion channels (ASICs; Kress and Zeilhofer, 1999) have been identified in dorsal root ganglion and brain neurons, which have varying activation and inactivation kinetics, ionic permeability and pH sensitivity. Recent evidence suggests that TRPV1 may combine with TRPV3 to form heteromeric capsaicin sensitive ion channels, resulting in functional and pharmacological diversity (Smith et al., 2002).

* Corresponding author. Tel.: +44 115 9513257; fax: +44 115 9513230.
E-mail address: ian.mellor@nottingham.ac.uk (I.R. Mellor).
[1] Present address: Department of Animal Physiology and Biophysics, Faculty of Biology, University of Bucharest, Splaiul Independentei 91-95, 76201 Bucharest, Romania.

0014-2999/$ - see front matter © 2004 Elsevier B.V. All rights reserved.
doi:10.1016/j.ejphar.2004.10.005

TRPV1 is well known for its high expression in nociceptive sensory neurons of dorsal root ganglia, but is also expressed at high levels in trigeminal ganglia, pancreas and taste papillae (Ishida et al., 2002), and at more moderate levels in numerous organs (Gunthorpe et al., 2002). Accordingly, TRPV1 is known to play a part in pain processing and transgenic mice lacking TRPV1 show impaired sensitivity to vanilloid and heat evoked pain (Caterina et al., 2000). TRPV1 is also implicated in diseases such as bladder and bowel dysfunction, and is thus a potential drug target.

Known ligands for TRPV1 include exogenous agonists such as capsaicin and its analogues, resiniferatoxin (Szallasi and Blumberg, 1989) and gingerols (Dedov et al., 2002); the endogenous agonists anandamide (Smart et al., 2000) and *N*-arachidonyl-dopamine (Huang et al., 2002); competitive antagonists for example capsazepine (Urban and Dray, 1991) and iodo-resiniferatoxin (Wahl et al., 2001; Seabrook et al., 2002); and non-competitive antagonists such as ruthenium red (Maggi et al., 1988) and trialkylglycine analogues (Garcia-Martinez et al., 2002). Recently, ethanol has been shown to activate TRPV1 as well as potentiate its responses to capsaicin, protons and heat (Trevisani et al., 2002). Furthermore, Babes et al. (2002) have shown that cooling can inhibit capsaicin-induced responses in rat dorsal root ganglion neurons.

In this study we have investigated the possibility that the polymethylene tetraamine, methoctramine, and some of its analogues can antagonize TRPV1 responses to capsaicin and protons, the aim being to assess their potential for the study of TRPV1 structure and binding sites or pharmaceutical development. Methoctramine is known as a competitive antagonist at muscarinic acetylcholine receptors with selectivity for the M_2 type and having a pK_B of 7.91 (Melchiorre et al., 1987; Rosini et al., 1999, 2002). It is also a non-competitive antagonist of nicotinic acetylcholine receptors having an IC_{50} of 1.2 μM on carbachol-induced frog rectus abdominus muscle contractions (Rosini et al., 1999, 2002). Methoctramine is a symmetrical molecule consisting of a linear tetraamine with 6-8-6 methylene spacing between the four secondary amine groups, and a 2-methoxybenzyl group attached at each end. Since it has been reported that polymethylene tetraamines, like spermine and homologs, are almost fully protonated at physiological pH (Aikens et al., 1983), it derives that methoctramine is polycationic at physiological pH, carrying most likely a charge of +4. This makes methoctramine and its analogues good candidates as TRPV1 antagonists based on the observation that the highly cationic ruthenium red is a non-competitive antagonist of the receptor, and this provides the rationale for this study. Furthermore, there is more scope for structural modification of methoctramine compared to ruthenium red. Many analogues have been synthesized, with generally reduced activity at muscarinic acetylcholine receptors, e.g. the analogues used in this study were all less potent than methoctramine by up to 1000 times (for compound 10); and variable activity at nicotinic acetylcholine receptors, e.g. the compounds used in this study ranged from ~10 times more potent (compound 7) to ~10 times less potent (compound 10) than methoctramine (Rosini et al., 1999, 2002). We show that on patch-clamped foetal and adult rat dorsal root ganglion neurons, methoctramine inhibits responses to capsaicin and protons in a voltage-dependent manner, and a range of analogues inhibit capsaicin responses with variable potency and voltage-dependence. This study has thus identified methoctramine and its analogues as a novel group of TRPV1 antagonists, and the relatively high voltage-dependence of some analogues make them useful tools to study and exploit a possibly unique binding site on the channel.

2. Methods

2.1. Foetal rat dorsal root ganglion preparation

Pregnant Wistar rats (Charles River, UK) were killed by anaesthesia and cervical dislocation as specified by national and institutional regulations, and approved by the institutional ethics committee. The foetuses were immediately decapitated upon dissection. Dorsal root ganglia were removed from 15-day-old foetus' and maintained in Leibovitz (L-15) medium (Gibco) on ice until enzymatic digestion. The ganglia were then placed in Hanks Balanced Salt Solution (Sigma) containing 0.25% trypsin (Worthington Biochemical Corporation) and incubated at 37 °C in a shaking water bath for 45 min. L-15 medium containing 20% foetal calf serum (Gibco) was then added to stop enzymatic digestion. Tissue was centrifuged (1000 rpm, 5 min), and the supernatant removed and replaced with fresh L-15 with 20% foetal calf serum. After trituration, the single cell suspension was centrifuged (1000 rpm, 5 min) and resuspended to 6×10^5 cells/ml in Eagle's Minimum Essential Medium (Sigma) with 10% foetal calf serum, 100 ng/ml mouse nerve growth factor 2.5S (Alomone Labs) and 5 mg/ml glucose (Sigma). Cells were plated as 30 μl drops onto glass coverslips and incubated overnight at 37 °C in a humidified 5% CO_2 atmosphere. Neurobasal medium (Gibco) with B27 serum free supplement (Gibco), 100 ng/ml mouse nerve growth factor 2.5 S, 5 mg/ml glucose and 0.298 mg/ml L-glutamine (Gibco) was added to the cultures the following day. Cells were used 1 or 2 days after plating for patch-clamp recording experiments.

2.2. Adult rat dorsal root ganglion preparation

Male Wistar rats (Charles River, UK) were killed by anaesthesia and cervical dislocation as specified by national and institutional regulations, and approved by the institutional ethics committee. Dorsal root ganglia were dissected

from 6- to 8-week-old rats and placed in filtered Ca^{2+}-free solution containing (in mM): 155 NaCl, 1.5 K_2HPO_4, 5.6 HEPES, 4.8 NaHEPES, 5 glucose, 50 μg/ml gentamicin, pH 7.5, until enzyme treatment. The ganglia were then incubated with an enzyme mixture of 3 mg/ml dispase and 1 mg/ml collagenase in Ca^{2+}-free solution for 1 h at 37 °C. After incubation the tissue was triturated in culture medium (Dulbecco's Modified Eagle Medium/Ham's F-12, supplemented with 10% horse serum and 50 μg/ml gentamicin) and then centrifuged for 10 min at 2000 rpm. The supernatant was removed and the cells resuspended in culture medium (100 μl per ganglion). They were plated on poly-L-lysine coated glass coverslips at a density of half a ganglion per coverslip and placed in an incubator (37 °C, 5% CO_2) to settle. After 2 h, 2 ml of culture medium was added to each dish. Cells were used 1 or 2 days after plating for patch-clamp recording experiments.

2.3. Patch-clamp recording

Whole-cell or outside-out patch-clamp was used to record responses of dorsal root ganglion neurons to 1–10 μM capsaicin (representing sub-saturating and saturating concentrations, respectively; the EC_{50} for capsaicin was 0.63 μM) or pH 5.4. Patch-clamp pipettes were pulled using a Sutter P-97 programmable pipette puller and had resistances of 5–10 MΩ when filled with a solution containing (in mM): CsCl 140, $CaCl_2$ 1, HEPES 5, EGTA 11, pH 7.2 with CsOH. Glass coverslips carrying dorsal root ganglion neurons were placed in a perfusion bath and constantly perfused (8 ml min^{-1}) with saline containing (in mM): NaCl 135, KCl 5.4, $CaCl_2$ 1, HEPES 5, $NaHCO_3$ 4, glucose 10, pH 7.4 with NaOH. To prepare pH 5.4 solution, HEPES was replaced by 2-[*N*-morpholino]ethanesulphonic acid (MES). Capsaicin, pH 5.4 and methoctramine analogues were applied using a DAD-12 drug application system (Adams and List Associates, New York, USA). Whole-cell patch-clamped dorsal root ganglion neurons were initially exposed to 1–10 μM capsaicin (or pH 5.4) for 10 s then the methoctramine analogue was added, increasing its concentration stepwise after every 10 s to the highest concentration (1–5 steps), then back to capsaicin (or pH 5.4) alone for the final 10 s of the application. Some currents in response to pH 5.4 were transient in nature. In this case the dorsal root ganglion neuron was exposed to pH 5.4 alone or with methoctramine (1–100 μM) as a 2-s pulse. Outside-out patches from dorsal root ganglion neurons were exposed to 1–10 μM capsaicin for 30 s, then capsaicin plus 3–30 μM methoctramine for 30 s, then back to capsaicin alone for 30 s. Responses were measured using an Axopatch 200 patch-clamp amplifier (Axon Instruments, USA) and recorded to the hard disk of a PC using pClamp 5.7.2 (whole-cell) or Axotape (single channel) software (Axon Instruments). Data recording and drug application were synchronized by means of a trigger pulse from pClamp to the DAD-12. Whole-cell data were plotted as % of control response (to capsaicin or pH 5.4 alone), and IC_{50}s±S.E.M. were estimated by fitting the following equation:

$$\%\ \text{control response} = \frac{100}{1 + \left(IC_{50}/[\text{Met}]^{S}\right)} \quad (1)$$

where [Met] is the concentration of the methoctramine analogue and *S* is the Hill Slope. Curve fitting was performed using GraphPad Prism 3.02 software. Single channel data were analysed using the WinEDR2.3.3 program (John Dempster, Department of Physiology and Pharmacology, University of Strathclyde, UK). All measurements were taken for *N* cells/patches. IC_{50} values obtained

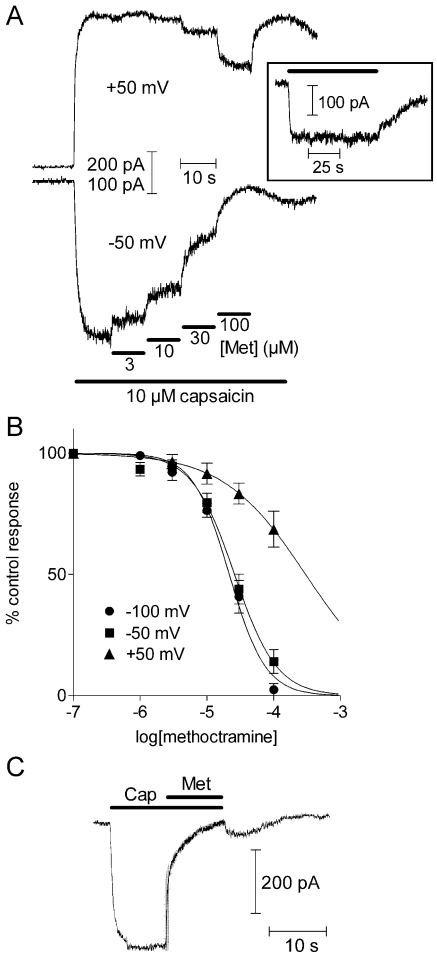

Fig. 1. Antagonism of capsaicin currents from foetal dorsal root ganglion neurons by methoctramine. (A) Whole-cell currents in response to 10 μM capsaicin from two dorsal root ganglion neurons clamped at +50 and −50 mV. After 10 s, 3 μM methoctramine (Met) was added and sequentially increased in concentration every 10 s up to 100 μM. The inset shows a response to a 70 s application of 10 μM capsaicin alone at –50 mV. (B) Concentration–inhibition curves for antagonism by methoctramine at –100 mV (●, *N*=7), –50 mV (■, *N*=10) and +50 mV (▲, *N*=8), for pooled data as shown in (A). The data are means±S.E.M. and are fitted by Eq. (1) (solid curves). The IC_{50} values are given in Table 1. (C) A double exponential decay fit (grey line) to the antagonizing phase of a response to 10 μM capsaicin (Cap, black line) following the addition of 100 μM methoctramine (Met) at –50 mV. The decay rates of the two components were 5.04 and 0.26 s^{-1} with relative spans of 0.55 and 0.45, respectively.

from curve fits were compared using F-tests and considered significantly different when $P<0.05$. Mean values of inhibition or single-channel parameters were compared using Student's t-tests and considered significantly different when $P<0.05$.

2.4. Materials

Methoctramine and its analogues were synthesized by standard procedures as described in Melchiorre et al. (1987, 1989), Minarini et al. (1989, 1991), Quaglia et al. (1991), and Rosini et al. (1999, 2002) and were characterized by IR, ^{1}H NMR, ^{13}C NMR, mass spectra and elemental analysis. All analogues were dissolved directly into the experimental saline solution and serially diluted. Ruthenium red was obtained from Sigma (Poole, Dorset, UK).

3. Results

3.1. Foetal rat dorsal root ganglion neurons

Whole-cell currents in response to 1–10 μM capsaicin were obtained in 63% of the foetal rat dorsal root ganglion neurons tested (N=1067). These currents rose within 10 s to a steady state that was maintained for the duration of its application (up to 70 s; Fig. 1A inset). None of the methoctramine analogues evoked a response when tested alone on dorsal root ganglion neurons responding to capsaicin.

3.1.1. Structure–activity relationship (SAR)

Methoctramine (**4**) and 16 of its analogues (Table 1) were tested for their ability to antagonize whole-cell responses of foetal dorsal root ganglion neurons to 10 μM capsaicin at

Table 1
Structures of methoctramine (**4**) and its analogues and their IC_{50} (±S.E.) values for inhibition of foetal dorsal root ganglion neuron whole-cell responses to 10 μM capsaicin

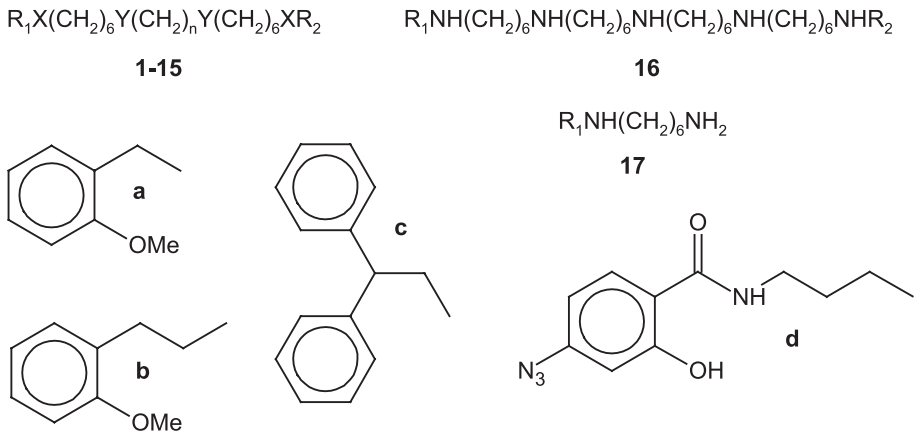

Compound	R_1	R_2	n	X	Y	IC_{50}±S.E. (N cells) at V_H (μM)		
						−100 mV	−50 mV	+50 mV
1	**a**	**a**	5	NH	NH	51.0±0.3 (6)	80.9±5.7 (10)	NSI (10)
2	**a**	**a**	6	NH	NH	12.3±1.9 (6)	18.4±3.5 (10)	128±13 (8)
3	**a**	**a**	7	NH	NH	11.7±3.5 (13)	29.2±6.7 (13)	>>100 (14)
4	**a**	**a**	8	NH	NH	21.7±2.0 (7)	26.0±1.1 (10)	304±9 (8)
5	**a**	**a**	10	NH	NH	16.0±4.8 (28)	27.2±2.4 (21)	>>100 (26)
6	**a**	**a**	11	NH	NH	13.5±2.4 (5)	28.2±4.2 (13)	328±42 (9)
7	**a**	**a**	12	NH	NH	7.10±0.99 (5)	11.6±0.8 (8)	104±20 (5)
8	**a**	**a**	14	NH	NH	~25 (lysis)	31.2±7.8 (7)	79.0±5.8 (6)
9	**a**	**a**	8	NCH_3	NCH_3	70.1±5.7 (6)	62.5±4.1 (8)	197±32 (9)
10	**a**	**a**	8	NH	O	35.5±5.8 (11)	14.5±2.2 (12)	39.5±2.2 (11)
11	**a**	H	8	NH	NH	9.18±0.57 (5)	12.7±1.6 (7)	NSI (6)
12	**d**	H	8	NH	NH	7.89±1.38 (7)	19.8±1.6 (15)	NSI (6)
13	H	H	8	NH	NH	>>100 (6)	>>100 (6)	>>100 (6)
14	**b**	**b**	8	NH	NH	16.0±2.8 (6)	19.0±1.8 (5)	NSI (6)
15	**c**	**c**	8	NH	NH	2.14±0.48 (8)	2.46±0.37 (14)	82.9±14.5 (5)
16	**a**	**a**				26.8±3.9 (8)	38.9±5.3 (12)	108±14 (10)
17	**a**					>>100 (6)	NSI (3)	NSI (8)
Ruthenium red						1.29±0.15 (3)	1.33±0.16 (7)	2.31±0.28 (8)

NSI=no significant inhibition. Values greater than 100 μM (highest analogue concentration tested) are estimates obtained by extrapolation of the fit of Eq. (1) to the data.

holding potentials (V_H) of +50, –50 and –100 mV. Concentration–inhibition relationships were obtained for each compound and resultant IC_{50} values are given in Table 1. Relative potencies (based on IC_{50} values) compared to **4** (=1) are illustrated in Fig. 2.

Methoctramine inhibited responses to 10 μM capsaicin (Fig. 1) with IC_{50}s of 21.7 μM (N=7), 26.0 μM (N=10) and 304 μM (N=8) at –100, –50 and +50 mV, respectively (Fig. 1B). Its action was voltage-dependent (Fig. 1A,B) with the IC_{50} being lower at more negative holding potentials. There was however some inhibition at +50 mV (Fig. 1A). Recovery from antagonism by methoctramine and its analogues was also voltage-dependent. Following inhibition by 100 μM methoctramine (for 10 s), application of 10 μM capsaicin alone for 10 s resulted in 19.2±10.3% (N=3), 45.9±5.3% (N=19) and 88.1±9.6% (N=4) recovery at –100, –50 and +50 mV, respectively (P=0.0028 for –50 mV vs. +50 mV). The onset of inhibition by 100 μM methoctramine at –50 mV was biphasic with fast and slow rates of 4.35±0.57 and 0.22±0.03 s^{-1} (N=16), and fractional contributions of 0.464±0.031 and 0.536±0.031, respectively (Fig. 1C).

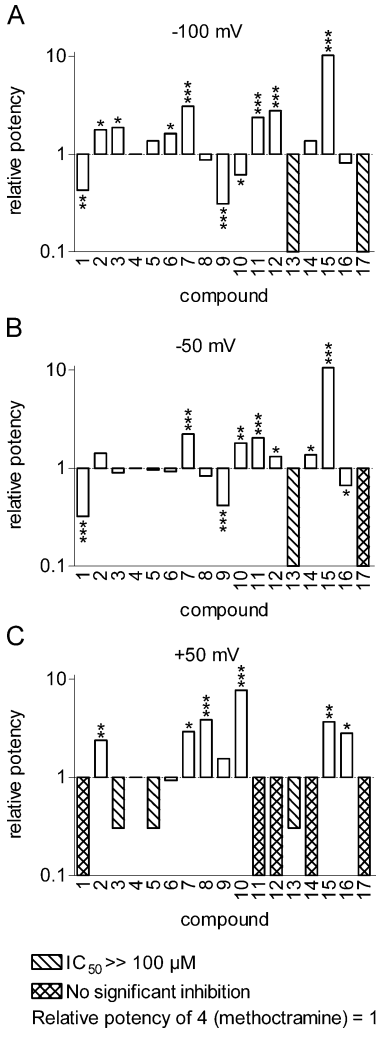

Fig. 2. Relative potencies of methoctramine analogues at −100 mV (A), −50 mV (B) and +50 mV (C) calculated by comparing their IC_{50} values for inhibition of capsaicin (10 μM) responses of foetal dorsal root ganglion neurons to that of methoctramine (**4**). Bars marked with diagonal lines indicate where the IC_{50} could not be calculated due to low potency, i.e. IC_{50}>>100 μM; bars marked with crossed lines indicate no significant inhibition. Significant changes in potency compared to methoctramine (**4**) are indicated by * (P<0.05), ** (P<0.01) or *** (P<0.001).

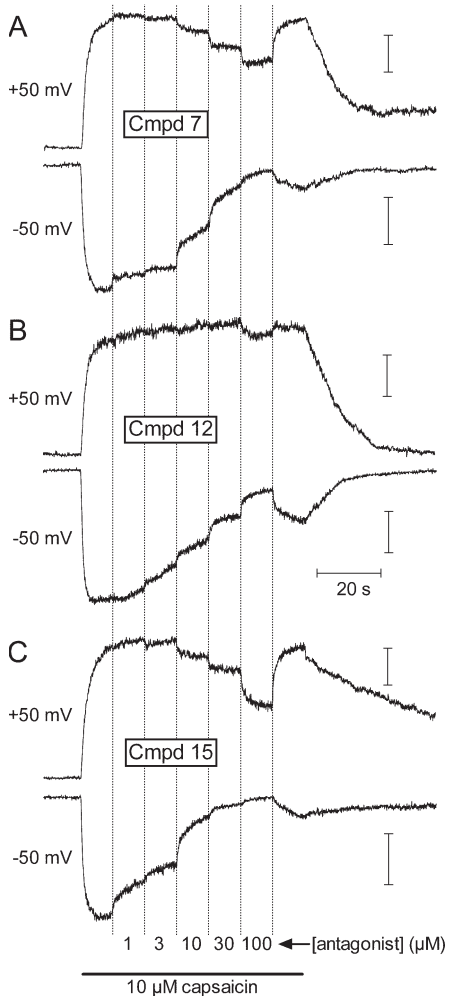

Fig. 3. Antagonism of capsaicin (10 μM) induced whole-cell currents from foetal dorsal root ganglion neurons by compounds **7** (A), **12** (B) and **15** (C). Antagonists were applied at concentrations of 1, 3, 10, 30 and 100 μM in continuous steps, each for 10 s. The vertical scale bars all represent 200 pA. Each response was from a different dorsal root ganglion neuron.

Compounds **1** to **8** were used to observe the effect of shortening or lengthening the central methylene chain (n=5–8, 10–12 and 14) of **4** (n=8) on antagonism. All of the compounds inhibited responses to 10 μM capsaicin in a voltage-dependent manner. Compared to **4**, at –50 mV (Fig. 2B), the shortest compound (**1**) was 3-fold less potent, **2** was slightly more potent (1.4-fold), **7** (Fig. 3A) was 2.2-times more potent, while **3**, **5**, **6** and **8** had similar potencies (all P>0.215). At –100 mV (Fig. 2A), again, **1** was less potent, **2** and **7** were more potent and **5** was similar in potency compared to **4**. In contrast to their potency at –50 mV, **3** and **6** were significantly more potent than **4** at –100 mV,

reflecting a higher dependence on V_H. Compound **8**, caused rapid lysis (as indicated by the loss of electrical seal) of the cells at –100 mV when applied at 100 μM and it was not possible to test the complete range of concentrations; single applications of 30 μM **8** caused 57.4±19.6% (N=3) inhibition, suggesting an estimated IC_{50} of ~25 μM, i.e. similar to **4**. At +50 mV (Fig. 2C), **2** and **7** (Fig. 3A) were more potent than **4**, and **6** was similarly potent. In contrast to its action at –50 mV, **8** was 3.8-times more potent than **4**, indicating a lower dependency on V_H. The other compounds in this group were less potent than **4** at +50 mV and **1** was inactive.

In compound **9**, all four amine groups of **4** were methylated, converting them from secondary to tertiary amines. This caused a 2- to 3-fold decrease in potency at –50 and –100 mV (Fig. 2A,B), but resulted in a similar potency at +50 mV (Fig. 2C). Again, this indicates a significant reduction in voltage-dependence of inhibition.

Replacing the two inner amine groups with ether groups (O) resulted in compound **10**, which thus carries a reduced charge of +2. This was slightly more potent than **4** at –50 mV (Fig. 2B), but much more potent at +50 mV (8.6-fold; Fig. 2C). Therefore, compound **10** seems to cause mostly voltage-independent inhibition, although the IC_{50} at –50 mV was still significantly lower (2.7-fold, P<0.0001) than at +50 mV. The IC_{50} at –100 mV was higher than for **4** and significantly increased compared to its value at –50 mV (P=0.0057), creating an unusual voltage/inhibition profile. However, like **8** but to a lesser extent, 100 μM **10** caused lysis of cells at –100 mV and leakage current may explain the higher IC_{50} at this V_H. Compound **10** was the most potent compound at +50 mV (Fig. 2C).

Removal of one of the aromatic end groups (**a**) of methoctramine gave compound **11** that has a free terminal amine group. This was significantly more potent than **4** at –100 mV (Fig. 2A) and –50 mV (Fig. 2B), but inactive at +50 mV (Fig. 2C). Inhibition by compound **11** was thus completely voltage-dependent. A similar compound with a differing aromatic 'head-group' (**d**), **12**, behaved almost identically. Its effect on capsaicin currents is shown in Fig. 3B. It was 2.8-times more potent than **4** at –100 mV (Fig. 2A), 1.3-times more potent at –50 mV (Fig. 2B), but inactive at +50 mV (Fig. 2C). However, removing both aromatic groups of **4** (**13**) resulted in a large drop in potency (Fig. 2). At –100, –50 and +50 mV only 17.3±6.4% (N=6), 21.9±6.4% (N=6) and 14.5±4.6% (N=6) inhibition was observed with 100 μM **13**. The weak inhibition was voltage-independent.

Compounds **14** and **15** were employed to test the effect of changing the end groups of methoctramine. Compound **14** has an additional methylene group between the 2-methoxybenzyl group and the outer amine group at both ends of the molecule (**b**). This compound was slightly more potent than **4** at negative V_H (Fig. 2A,B), but this was only statistically significant at –50 mV. At +50 mV, **14** was inactive. In compound **15**, the 2-methoxybenzyl group (**a**) was changed for a larger group (**c**). This compound was considerably more potent than **4** (Fig. 2); 10.1-fold at –100 mV, 10.6-fold at –50 mV and 3.7-fold at +50 mV (Fig. 3C). The greater increase in potency at negative V_H indicates a greater contribution of voltage-dependent inhibition, although **15** was still quite active at +50 mV. **15** was the most potent compound tested at –100 and –50 mV.

Elongation of methoctramine with addition of an amine group gave the pentaamine **16**. This was slightly less potent than **4** at –100 and –50 mV (Fig. 2A,B). However, at +50 mV (Fig. 2C) it was 2.8-times more potent. In other words it was less voltage-dependent in its action compared to **4**.

Finally, a short diamine analogue of methoctramine, compound **17**, was tested. This caused minor antagonism at –100 mV (18.8±4.5%, N=6, by 100 μM **17**), but was inactive at –50 and +50 mV.

For comparison we analysed the effect of ruthenium red using the same protocol (Table 1). It was 17-fold, 20-fold

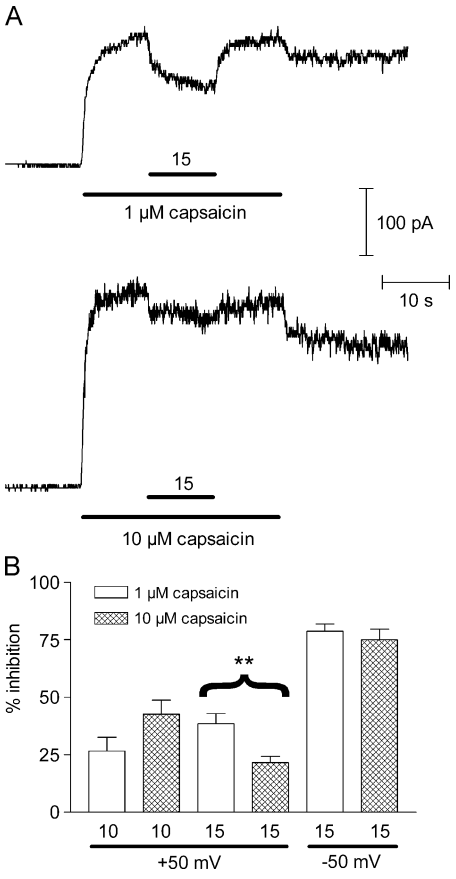

Fig. 4. The effect of capsaicin concentration on antagonism by compounds **10** and **15**. (A) Whole-cell currents from two foetal dorsal root ganglion neurons exposed to 1 μM (upper trace) or 10 μM (lower trace) capsaicin at +50 mV. Compound **15** was applied at a concentration of 10 μM for 10 s during the capsaicin application. (B) Mean inhibition by compounds **10** (at +50 mV) and **15** (at +50 and −50 mV) of foetal dorsal root ganglion neuron responses to 1 or 10 μM capsaicin. Bars indicate mean±S.E.M. for N (from left to right)=12, 17, 16, 16, 17 and 25 cells. The difference between the means for **15** at +50 mV is highly significant (**).

and 132-fold more potent than **4** at –100, –50 and +50 mV, respectively. Compared to **15**, the most potent methoctramine analogue, ruthenium red was slightly more potent (1.7 to 1.8-times) at –100 and –50 mV, but considerably more potent (36-times) at +50 mV (Table 1). This is because ruthenium red exhibited very little voltage-dependence in its action.

3.1.2. Dependence of [capsaicin]

Compounds **10** and **15** showed a reasonable level of antagonism at +50 mV, which could be attributed to non-competitive closed-channel block or to competitive antagonism (either directly or allostericaly). **10** (30 μM) or **15** (10 μM) were co-applied during responses of foetal rat dorsal root ganglion neurons to either 1 μM or 10 μM capsaicin at

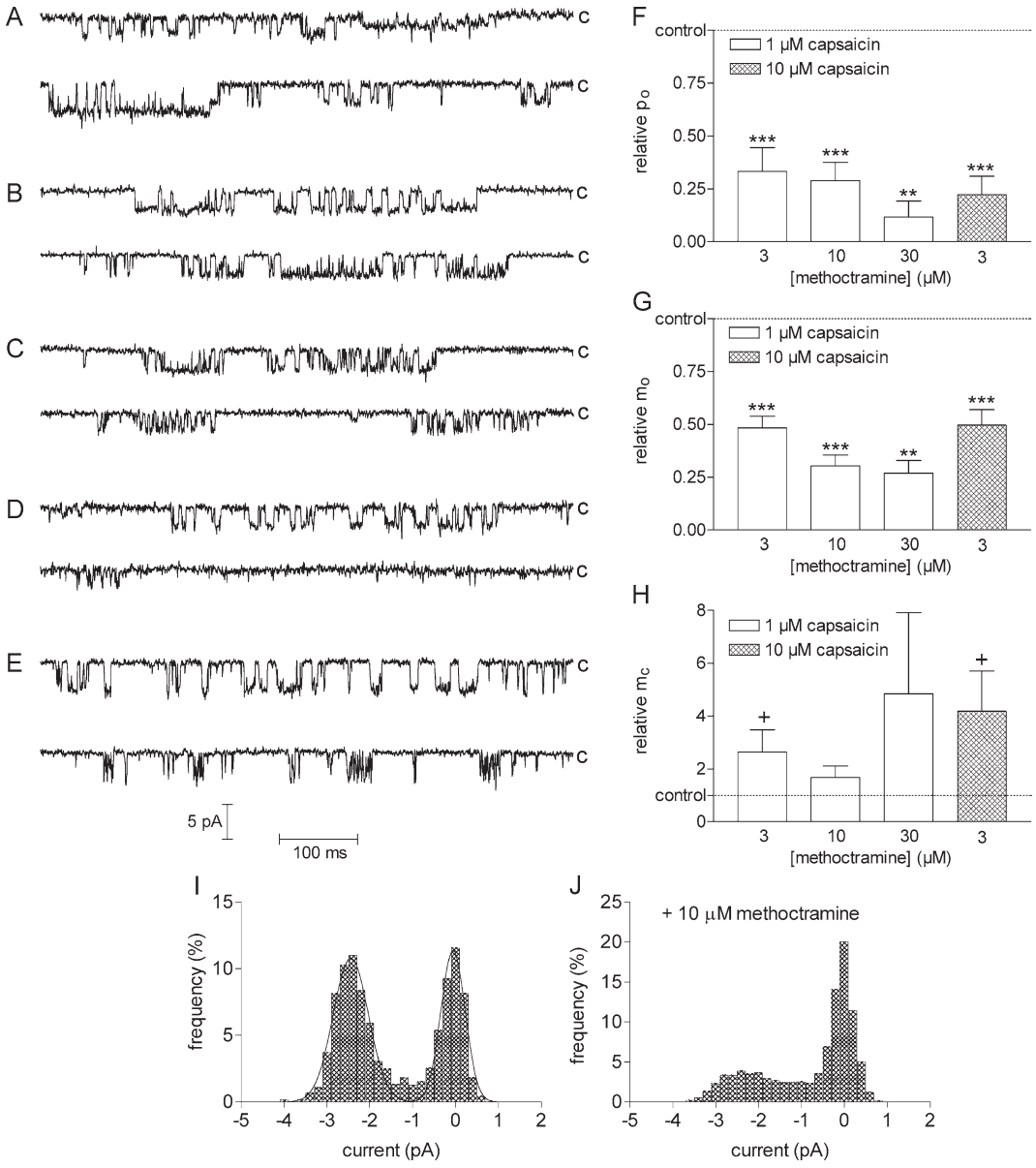

Fig. 5. Single channel studies with outside-out patches from foetal dorsal root ganglion neurons. All recordings were at −60 mV. (A) Two patches exposed to 1 μM capsaicin showing the 22.7 pS subconductance (upper trace) and the 64.3 pS higher conductance (lower trace) alongside the normal 39.9 pS conductance. (B−D) Three patches exposed to 1 μM capsaicin in the absence (upper trace) and presence (lower trace) of 3 μM (B), 10 μM (C) or 30 μM (D) methoctramine, showing concentration-dependent 'flickery' block. (E) A patch exposed to 10 μM capsaicin predominantly showing the high conductance (64.3 pS), in the absence (upper trace) and presence (lower trace) of 3 μM methoctramine. The closed state for each trace is indicated by 'c'. (F−H) Bar graphs respectively showing p_o, m_o and m_c in the presence of 3, 10 and 30 μM methoctramine relative to their control values (=1 in each case). The bars are means±S.E.M. for N (from left to right)=6, 6, 2 and 5. Significant differences from the control values are indicated by * (P<0.05), ** (P<0.01) and *** (P<0.001), and P<0.1 is indicated by +. (I−J) All points histograms from a patch exposed to 1 μM capsaicin in the absence (I) and presence (J) of 10 μM methoctramine. The histogram in (I) has been fitted with the sum of two Gaussian distributions with peak separation of 2.38 pA, giving a single channel conductance of 39.7 pS in this patch. The histograms were prepared from a single burst of openings in each case to enhance the open state peak.

+50 mV (at this V_H, any voltage-dependent inhibition should be absent) (Fig. 4A). Compound **10** (30 μM) caused 26.7±6.0% (N=12) inhibition of responses to 1 μM capsaicin and 42.7±6.0% (N=17) inhibition of responses to 10 μM capsaicin (Fig. 4B). Although not statistically significant (P=0.079), the data indicate that if anything, **10** is slightly more potent against responses to 10 μM capsaicin, and is thus not competing with capsaicin. Compound **15** (10 μM) caused 38.5±4.4% (N=16) inhibition of responses to 1 μM capsaicin and 21.6±2.7% (N=16) inhibition of responses to 10 μM capsaicin (Fig. 4B). Inhibition was significantly greater in the presence of 1 μM capsaicin indicating that 15 and capsaicin may compete directly or allosterically for the agonist-binding site, but if so this is a minor component of the overall inhibition. The experiment was repeated at –50 mV with **15** (Fig. 4B). At this V_H antagonism of responses to 10 μM capsaicin (84.9±4.7%, N=25) was virtually as much (P=0.56) as that of responses to 1 μM capsaicin (88.7±3.2%, N=17).

3.1.3. Single-channel experiments

Application of 1 or 10 μM capsaicin to outside-out patches evoked bursts of channel openings with a mean conductance of 39.9±1.0 pS (N=36 patches) at –60 mV (Fig. 5); close to that determined in other studies with dorsal root ganglion neurons (Oh et al., 1996; Premkumar et al., 2002) and TRPV1 expressed in human embryonic kidney (HEK-293) cells (Caterina et al., 1997) or *Xenopus* oocytes (Premkumar et al., 2002). In 17 of these patches a subconductance of 22.7±0.6 pS was observed, contributing up to ~10% of the total open time (Fig. 5A). In seven patches a higher conductance of 64.3±0.6 pS was also seen, contributing up to ~20% of the total open time (Fig. 5A) and in 4 out of 12 patches exposed to 10 μM capsaicin at –60 mV, the higher conductance dominated (Fig. 5E). These additional conductances were also identified by Premkumar et al. (2002). No channel openings were seen in the absence of capsaicin. With 1 μM capsaicin the open probability (p_o) was 0.101±0.026 (N=15), the mean open time (m_o) was 3.52±0.38 ms (N=15) and the mean closed time (m_c) was 67.3±13.9 ms (N=15). Because of variation in m_c, and thus p_o, from patch-to-patch, p_o, m_o and m_c were normalized to the control values for each patch in order to compare these parameters in the presence of methoctramine, averaged for numerous patches (Table 2 and Fig. 5F–H). With 1 μM capsaicin there was a concentration dependent decrease in p_o and m_o, seen as 'flickery' block, consistent with open channel block (Fig. 5B–D,F,G). However, m_c consistently increased (but not statistically significant; P all ≥0.079) in all cases, although the concentration dependence was complex (Fig. 5H). This probably resulted from a balance between increased m_c via closed channel block and the introduction of some brief closing events caused by open channel block. With 10 μM capsaicin, 3 μM methoctramine reduced m_o to the same extent as with 1 μM capsaicin (Table 2, Fig. 5G), but overall, p_o was even less than with 1 μM capsaicin (Table 2, Fig. 5F) because of a greater increase in m_c (Table 2, Fig. 5H), showing that inhibition was non-competitive. Methoctramine (3 μM) had the same effect on the larger conductance channel openings (Fig. 5E). The all-points histograms shown in Fig. 5I and J show that the single channel current amplitude was not affected by 10 μM methoctramine, although the open channel peak was smeared towards the closed channel peak in the presence of methoctramine. This was caused by the more rapid flickering between the open and closed state and is further evidence for open-channel block.

3.1.4. Inhbition of responses to protons

Protons (pH 5.4) activated two types of current. The first had slow activation kinetics and a persistent current, like that evoked by capsaicin (sustained; Fig. 6A), and the current reversed close to 0 mV. The second type had more rapid activation (time-to-peak=289±15 ms, N=40) and desensitisation (decay rate=0.71±0.06 s^{-1}, N=40) kinetics (transient; Fig. 6C). At +50 mV, small inward transient currents were observed indicating a reversal potential more positive than +50 mV and thus selective permeability of Na^+ or Ca^{2+} ions. Additionally, transient currents were antagonized by 10 μM amiloride by 61.3±6.9% (N=11). Amiloride is known to block ASICs and closely related epithelial Na^+ selective ion channels (Waldmann et al., 1997). The data imply that these are ASIC mediated currents that are impermeable to Ca^{2+} (Zeilhofer et al., 1997), but selectively permeable to Na^+ (Kress and Zeilhofer, 1999) and blocked by amiloride. Out of all the proton-activated currents at –50 mV, 39% were of the sustained type, 37% were of the transient type and 24% were a combination of the two types (N=72). The latter appeared to be two separate currents because at +50 mV the transient component was reduced to a small inward current (like ASICs), while the sustained current was an outward current (like TRPV1). For cells tested with both pH 5.4 and capsaicin, all those giving a sustained pH 5.4 response also responded

Table 2
Single channel parameters in the presence of methoctramine (Met) expressed as mean values (±S.E.M.) relative to their controls in its absence

[Cap] (μM)	[Met] (μM)	Relative values ±S.E.M. (N patches)		
		p_o	m_o	m_c
1	3	0.332±0.113 (6)	0.484±0.055 (6)	2.64±0.84 (6)
1	10	0.288±0.087 (6)	0.303±0.052 (6)	1.67±0.44 (6)
1	30	0.117±0.076 (2)	0.269±0.059 (2)	4.84±3.07 (2)
10	3	0.222±0.087 (5)	0.497±0.073 (5)	4.18±1.52 (5)

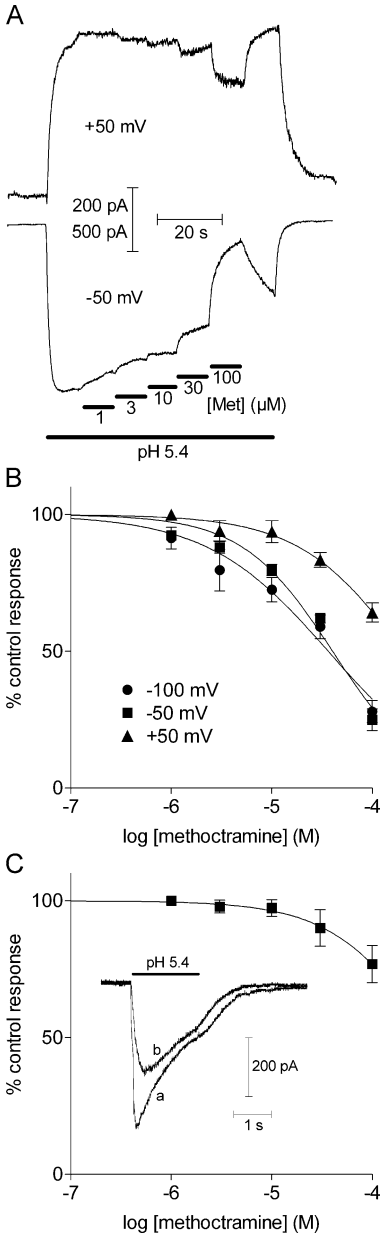

Fig. 6. Antagonism of foetal dorsal root ganglion neuron responses to pH 5.4. (A) Sustained whole-cell currents elicited by pH 5.4 from two dorsal root ganglion neurons clamped at +50 and −50 mV. After 10 s, 1 μM methoctramine (Met) was added and sequentially increased in concentration every 10 s up to 100 μM. (B) Concentration−inhibition curves for antagonism by methoctramine at −100 mV (●, N=5), −50 mV (■, N=7) and +50 mV (▲, N=8), for pooled data as shown in (A). The data are means±S.E.M. and are fitted by Eq. 1 (solid curves). The IC_{50} values are given in Table 3. (C) Transient whole-cell currents from a single dorsal root ganglion neuron in response to 2 s steps in pH from 7.4 to 5.4 (inset) in the absence (a) and presence (b) of 100 μM methoctramine. The concentration−inhibition data is pooled (mean±S.E.M.) from seven cells and is fitted by Eq. (1) (solid curve) to give an IC_{50} of 378±51 μM.

to capsaicin, while those that did not give a sustained response to pH 5.4 did not respond to capsaicin (N=39).

Sustained (only) currents were inhibited by methoctramine (Fig. 6A) with IC_{50}s of 36.5 μM (N=5), 40.3 μM (N=7) and 204 μM (N=8) at –100, –50 and +50 mV respectively (Fig. 6B). Thus, compared to inhibition of capsaicin induced currents (Table 3), methoctramine was slightly less potent at negative V_H and slightly more potent at +50 mV resulting in a less voltage-dependent antagonism. Transient currents were only poorly inhibited by methoctramine. At – 50 mV, the estimated IC_{50} for inhibition of the peak current (Fig. 6C) was 378±51 μM (N=7). The time-to-peak of the responses was increased significantly from 182±30 to 322±39 ms (P=0.0132, N=7) by 100 μM methoctramine. The rate of decay of the currents was also slowed by 100 μM methoctramine from 0.98±0.23 to 0.51±0.09 s^{-1} (P=0.0492, N=6). This indicates that methoctramine slows down both the activation and desensitisation kinetics (Fig. 6C).

3.2. Adult rat dorsal root ganglion neurons

3.2.1. Potency of methoctramine

Methoctramine (**4**) was compared for potency against responses of adult rat dorsal root ganglion neurons to 10 μM capsaicin (Fig. 7A, Table 3). The IC_{50} was almost identical at –100 mV, but was 1.9-fold higher at –50 mV and similar at +50 mV, when compared to equivalent measurements on foetal rat dorsal root ganglion neurons. At –50 mV the IC_{50} obtained in the presence of 1 μM capsaicin was not significantly different (P=0.907) from that obtained with 10 μM capsaicin (Fig. 7B and Table 3). This shows that methoctramine and capsaicin binding is non-competitive.

As with foetal dorsal root ganglion neurons, compound **15** was a significantly more potent antagonist of responses to 10 μM capsaicin than methoctramine, with IC_{50}s of 4.56±0.29 μM (N=9, P<0.0001) and 32.8±2.7 μM (N=7, P<0.0001) at –50 and +50 mV respectively. Compared to data from foetal dorsal root ganglion neurons, **15** was 1.9-times less potent (P=0.0069) at –50 mV, but 2.5 times more potent (P=0.0004) at +50 mV; less voltage-dependent than with foetal dorsal root ganglion neurons.

3.2.2. Inhibition of responses to protons

As noted with foetal dorsal root ganglion neurons, steps to pH 5.4 resulted in two types of whole-cell current, one that remained stable for the duration of the pH 5.4 application (sustained; Fig. 7C) and another that rapidly peaked at a rate of 34.8±2.9 s^{-1} and decayed at a rate of 1.22±0.05 s^{-1} (transient; Fig. 7D). At –50 mV, 73% were of the sustained type while 27% were of the transient type (N=15). At +50 mV all were of the sustained type (N=9), probably because the transient currents exhibit a reversal potential close to +50 mV (see above). Both types of current were inhibited by methoctramine. The IC_{50} for inhibition of sustained currents by methoctramine (Fig. 7C, Table 3) was similar to inhibition of capsaicin-evoked currents at –50 mV but more potent at +50 mV. The antagonism of responses to pH 5.4 was thus not as voltage-dependent compared to that

Table 3
IC_{50} (±S.E.) values for methoctramine inhibition of responses to capsaicin or pH 5.4 (sustained and transient) in foetal and adult dorsal root ganglion neurons

Dorsal root ganglion neuron	Agonist (current)	IC_{50}±S.E. (*N* cells) at V_H (μM)		
		−100 mV	−50 mV	+50 mV
Foetal	10 μM capsaicin	21.7±2.0 (7)	26.0±1.1 (10)	304±9 (8)
	pH 5.4 (sustained)	36.5±6.6 (5)	40.3±6.4 (7)	204±33 (8)
	pH 5.4 (transient)		378±51 (7)	
Adult	10 μM capsaicin	20.9±1.9 (6)	49.2±5.3 (16)	233±47 (4)
	1 μM capsaicin		47.8±6.3 (16)	
	pH 5.4 (sustained)		42.1±3.0 (6)	112±23 (5)
	pH 5.4 (transient)		193±32 (4)	

Values greater than 100 μM (highest methoctramine concentration tested) are estimates obtained by extrapolation of the fit of Eq. (1) to the data.

of capsaicin responses. Compared to inhibition of sustained pH 5.4 currents in foetal dorsal root ganglion neurons (Table 3), the IC_{50} was almost identical at –50 mV but 1.8-fold lower at +50 mV. For transient currents (–50 mV only) the IC_{50} was 193 μM (*N*=4); less potent than for stable pH 5.4 and capsaicin evoked currents of adult dorsal root ganglion neurons, but more potent than for inhibition of transient currents of foetal dorsal root ganglion neurons (Table 3). In accordance with foetal dorsal root ganglion neurons, the rising rate of transient currents was decreased (*P*=0.0034) by 100 μM methoctramine from 34.8±2.9 to 18.1±1.0 s^{-1} (*N*=4), and the rate of decay of the current was also decreased (*P*=0.0001) from 1.22±0.05 to 0.80±0.04 s^{-1} (*N*=4).

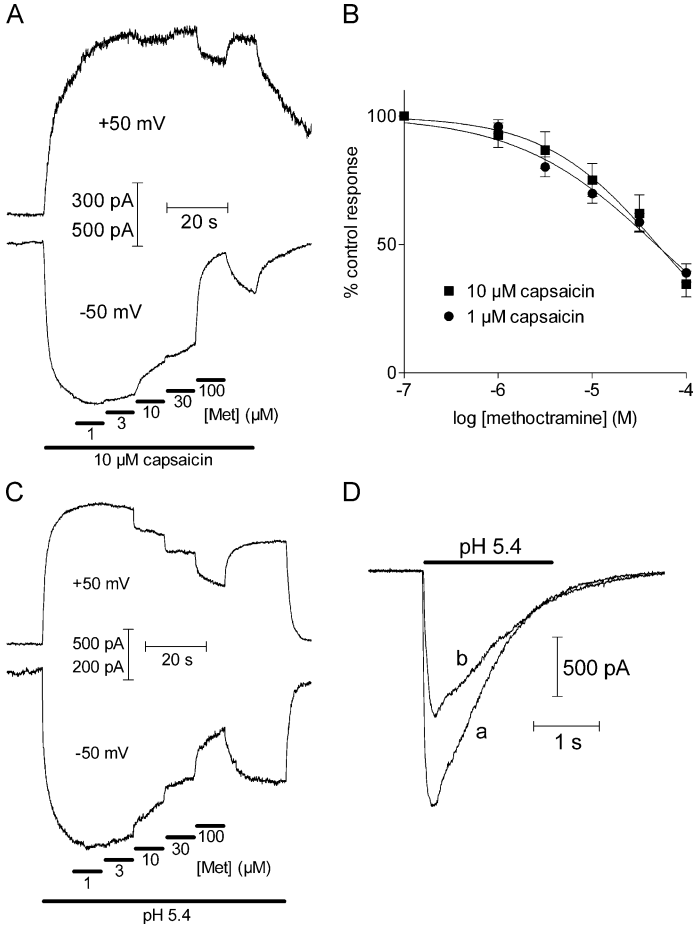

Fig. 7. Antagonism of responses of adult dorsal root ganglion neurons to capsaicin and pH 5.4. (A) Whole-cell currents in response to 10 μM capsaicin from two dorsal root ganglion neurons clamped at +50 and −50 mV. After 10 s, 1 μM methoctramine (Met) was added and sequentially increased in concentration every 10 s up to 100 μM. (B) Methoctramine concentration−inhibition curves for inhibition of responses to 10 μM (■, *N*=16) or 1 μM capsaicin (●, *N*=4) at −50 mV. All data are means±S.E.M. and are fitted by Eq. (1) (solid curves). The IC_{50} values are given in Table 3. (C) Sustained whole-cell currents elicited by pH 5.4 from two dorsal root ganglion neurons clamped at +50 and −50 mV. After 10 s, 1 μM methoctramine (Met) was added and sequentially increased in concentration every 10 s up to 100 μM. (D) Transient whole-cell currents from a single dorsal root ganglion neuron in response to 2 s steps in pH from 7.4 to 5.4 in the absence (a) and presence (b) of 100 μM methoctramine.

4. Discussion

4.1. Mechanism of antagonism

We have shown that methoctramine (**4**) is a non-competitive antagonist of dorsal root ganglion neuron responses to capsaicin, with very similar action in foetal and adult preparations. Since TRPV1 is currently the only protein identified in dorsal root ganglion neurons that binds capsaicin, it is reasonable to assume that methoctramine is an antagonist of TRPV1. The antagonism and recovery is voltage-dependent, suggesting that methoctramine is an open-channel blocker. However, there is clearly some antagonism of outward capsaicin evoked current (at +50 mV) suggesting that the binding site may be situated at a relatively shallow position in the pore. Alternatively, this voltage-independent component may result from the binding of methoctramine to a second site on TRPV1 causing closed-channel block. Support for this latter suggestion arises from the single channel studies. The reduction of m_o by methoctramine clearly indicates open-channel block, but the increase in m_c suggests a small additional closed channel blocking component. Also the biphasic onset of inhibition suggests the involvement of two modes of action. However, it remains that the major component appears to be voltage-dependent open-channel block.

Few open-channel blockers of TRPV1 have previously been identified. Ruthenium red (Maggi et al., 1988), which is a large highly charged (+6) cation is one well-known example, but only recently accepted as an open-channel blocker (Garcia-Martinez et al., 2000; Szallasi and Di Marzo, 2000). Our data showing that there was little voltage-dependence of antagonism by ruthenium red, suggest that its binding site is very shallow in the TRPV1 channel pore. Arginine-rich peptides of synthetic or natural origin cause weakly voltage-dependent inhibition and may bind at a very shallow site in the pore or at its entrance (Planells-Cases et al., 2000). Similarly, at physiological pH, methoctramine is highly charged (+4), but in contrast, these charges are distributed along a carbon chain of considerable length, and parts of the molecule may be able to penetrate deeper into the pore.

Models of TRPV1 transmembrane topology predict that several acidic residues (D646, E648 and E651) are situated at the extracellular mouth of the pore between the pore loop (P-loop) and the sixth transmembrane segment (TM6), and an additional glutamate in the P-loop (E636) is at the intracellular mouth (Fig. 8). There are also numerous acidic residues in the other relatively small extracellular loops that will be in close proximity to the mouth of the pore. These acidic residues are likely candidates as binding sites for polycationic channel blockers including those described herein, although there are also S, T and N residues in the P-loop which may hydrogen bond to amino groups. Mutation of E636 and D646 has recently been shown to affect TRPV1 sensitivity to ruthenium red (Garcia-Martinez et al., 2000).

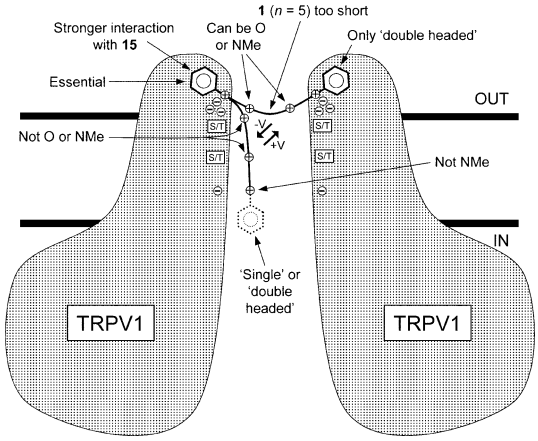

Fig. 8. Cartoon of a TRPV1 receptor showing speculative binding sites for methoctramine and its analogues. Acidic residues such as E636, D646, E648 and E651 are indicated by ⊖.

Additionally, a tyrosine residue (Y671) in TM6 has been shown to control Ca^{2+}-permeability of TRPV1 (Mohapatra et al., 2003) and may represent another potential site of action; there is a strong correlation between Ca^{2+}-permeability and block by polyamine-containing compounds in other ionotropic receptors (Mellor and Usherwood, 2004; Strømgaard and Mellor, 2004). Our continuing work will assess some of these predictions by using site-directed mutagenesis of TRPV1.

The widely spaced amino groups of methoctramine may be able to interact simultaneously with multiple nucleophilic residues on one TRPV1 subunit or multiple subunits (Fig. 8). A possible binding mode for voltage-independent inhibition may involve the 'strapping' together of some or all of the 4 TRPV1 subunits (Kedei et al., 2001) such that movements leading to channel gating are restricted; this is also highly dependent on two distal aromatic groups (Fig. 8). The entirely voltage-dependent antagonism caused by **11** and **12** (with only one aromatic endgroup) suggests that these compounds interact exclusively with residues deep inside the pore (Fig. 8). Conversely, **10** which contains oxygen atoms in the polyamine chain is less able to interact in the pore presumably due to its more electronegative properties.

The relatively slow recovery from inhibition by 100 μM methoctramine is perhaps surprising given the inhibitory potency of this compound. However, this may be due to the phenomenon of 'trapping' that is characteristic for open channel blockers, e.g. recovery of α-amino-3-hydroxy-5-methyl-4-isoxazole propionic acid (AMPA) receptors from inhibition by philanthotoxins is also very slow and can only be fully achieved by depolarising the cell in the presence of agonist (Mellor et al., 2003).

It is likely that the sustained currents evoked by pH 5.4 in dorsal root ganglion neurons are due to activation of TRPV1, since recombinant TRPV1 produce such responses when protons are applied (see e.g. Welch et al., 2000) and other proton activated sustained currents in dorsal root

ganglion neurons require a reduction to ≤pH 5.0 (Kress and Zeilhofer, 1999). Additionally we showed that all dorsal root ganglion neurons giving sustained responses to pH 5.4 also responded to capsaicin, and those not giving a sustained response to pH 5.4 did not respond to capsaicin. Antagonism of sustained proton responses by methoctramine was similar in foetal and adult dorsal root ganglion neurons, and was close to that observed for antagonism of capsaicin responses. There was however a reduction in the voltage-dependence of antagonism of proton responses compared to capsaicin responses that may be explained by methoctramine binding to a site outside the membrane electric field with higher affinity, or under proton activation the pore site is shifted to a more extracellular position. Either way it implies that the open state structure of TRPV1 differs following activation by capsaicin or protons, as previously suggested by Welch et al. (2000).

The transient proton activated currents were most likely due to ASIC activation because they were antagonized by amiloride and had a current–voltage relationship characteristic of ASICs. These currents were only weakly inhibited by methoctramine. The rate of rising to the peak and the rate of decay of the responses were reduced, suggesting that methoctramine may bind to ASICs to slow down their activation and desensitisation kinetics.

Compared to a number of other compounds that have been identified as antagonists of TRPV1, methoctramine analogues are of relatively low potency, but contribute to the limited list of TRPV1 open channel blockers. The methoctramine analogues tested thus far are probably not sufficiently potent to be considered as potential analgesics, and their actions at TRPV1 are still similarly or less potent than at muscarinic and nicotinic acetylcholine receptors, but, they may provide a new strategy for the design of such drugs. They do, however, appear to be potentially useful as tools to study TRPV1, as they have with nicotinic acetylcholine receptors (Bixel et al., 2001). Due to the unique highly voltage-dependent action compared to e.g. ruthenium red, methoctramine analogues may be used to probe the more intracellular parts of the channel pore.

In the single channel studies, methoctramine appeared to be a more potent antagonist of TRPV1 by about 10 times, when compared to whole-cell studies. One possibility is that higher tension in membrane patches as compared to whole cells, changes the structural properties of the TRPV1 such that it is more susceptible to methoctramine, possibly because channel open times are increased. Indeed, another member of the TRPV family, TRPV4, is activated by osmotic pressure presumably via membrane stretch. Alternatively, intracellular factors most likely to be present with whole-cell recording may affect the state of TRPV1.

4.2. Structure–activity study

Varying the central alkyl chain length between 6 and 11 methylenes (**2–6**) had little effect on antagonistic potency. Reducing the chain length to 5 methylenes (**1**) caused a drop in potency possibly because this molecule is now too short to bridge two essential points of contact (Fig. 8). Increasing the chain length to 12 methylenes (**7**) caused a small increase in potency at all V_H suggesting that this improvement was due to an increase in voltage-independent antagonism at a site outside the membrane electric field. A further increase to 14 methylenes (**8**) increased further the voltage-independent antagonism (at +50 mV), but reduced the voltage-dependent antagonism (at –50 mV). This longer more hydrophobic molecule may fold to a conformation that is favourable for a site outside the pore but perhaps too large to enter it.

Methylating the amino groups of methoctramine (**9**) reduced the voltage-dependent but not voltage-independent antagonism when compared to **4**. This suggests that **9** is less able to interact with the TRPV1 pore because of the increased bulk of the polyamine chain and possibly because the methyl groups hinder hydrogen bonding to hydrophilic residues (Fig. 8). Similarly, removing the two inner positively charged groups of **4** in favour of oxygen (**10**) greatly reduced its interaction in the pore.

Removal of one 2-methoxybenzyl group from **4** produced a compound (**11**) which was more potent at negative V_H but inactive at +50 mV. In other words, two aromatic groups are required for voltage-independent antagonism, but one aromatic group and a terminal amino group is favourable for binding deep in the pore (Fig. 8). This is fully supported by the related compound (**12**). However, at least one aromatic group is essential for activity since the unsubstituted 6-8-6 polyamine chain (**13**) caused only weak voltage-independent inhibition.

Compound **14** had an additional methylene group spacing the aromatic groups from the outer amino groups compared to **4**. This had little effect on antagonism at negative V_H but reduced activity at +50 mV such that it was entirely voltage-dependent. Clearly the spacing between the outer amino and aromatic groups is essential with regard to voltage-independent antagonism. Another change to the end groups of **4** caused the most pronounced increase in potency. Substituting the 2-methoxybenzyl groups for 2,2-dibenzylethyl (**15**) cause a three-fold increase in potency at +50 mV and approximately a ten-fold increase at –50 and –100 mV. Thus, both voltage-dependent and voltage-independent antagonism was improved with this compound.

Elongating and simultaneously increasing the charge to +5 (**16**) caused a small shift towards voltage-independent antagonism, while splitting the symmetrical methoctramine molecule adjacent to the inner amino groups (**17**) resulted in a compound that could not block the channels by any mechanism, presumably due to insufficient length, charge or both.

4.3. Conclusion

Based on the data presented, polyamine based compounds may be worth pursuing further with regard to the development of TRPV1 antagonists with pharmaceutical potential. These data certainly provide a basis for further studies of polyamines on cloned and mutant TRPV1 that will give more insight into its binding sites and structure.

Acknowledgements

The work was partially funded by donation from the FRAME research program.

References

Aikens, D., Bunce, S., Onasch, F., Parker III, R., Hurwitz, C., Clemans, S., 1983. The interactions between nucleic acids and polyamines: II. Protonation constants and ^{13}C NMR chemical shift assignments of spermidine, spermine, and homologs. Biophys. Chemist. 17, 67–74.

Babes, A., Amuzescu, B., Krause, U., Scholz, A., Flonta, M.L., Reid, G., 2002. Cooling inhibits capsaicin-induced currents in cultured rat dorsal root ganglion neurones. Neurosci. Lett. 317, 131–134.

Benham, C.D., Gunthorpe, M.J., Davis, J.B., 2003. TRPV channels as temperature sensors. Cell Calcium 33, 479–487.

Bixel, M.G., Weise, C., Bolognesi, M.L., Rosini, M., Brierley, M.J., Mellor, I.R., Usherwood, P.N.R., Melchiorre, C., Hucho, F., 2001. Location of the polyamine binding site in the vestibule of the nicotinic acetylcholine receptor ion channel. J. Biol. Chem. 276, 6151–6160.

Caterina, M.J., Julius, D., 2001. The vanilloid receptor: a molecular gateway to the pain pathway. Annu. Rev. Neurosci. 24, 487–517.

Caterina, M.J., Schumacher, M.A., Tominaga, M., Rosen, T.A., Levine, J.D., Julius, D., 1997. The capsaicin receptor: a heat-activated ion channel in the pain pathway. Nature 389, 816–824.

Caterina, M.J., Leffler, A., Malmberg, A.B., Martin, W.J., Trafton, J., Petersen-Zeitz, K.R., Koltzenburg, M., Basbaum, A.I., Julius, D., 2000. Impaired nociception and pain sensation in mice lacking the capsaicin receptor. Science 288, 306–313.

Dedov, V.N., Tran, V.H., Duke, C.C., Connor, M., Christie, M.J., Mandadi, S., Roufogalis, B.D., 2002. Gingerols: a novel class of vanilloid receptor (VR1) agonists. Br. J. Pharmacol. 137, 793–798.

Garcia-Martinez, C., Morenilla-Palao, C., Planells-Cases, R., Merino, J.M., Ferrer-Montiel, A., 2000. Identification of an aspartic residue in the P-loop of the vanilloid receptor that modulates pore properties. J. Biol. Chem. 275, 32552–32558.

Garcia-Martinez, C., Humet, M., Planells-Cases, R., Gomis, A., Caprini, M., Viana, F., De La Pena, E., Sanchez-Baeza, F., Carbonell, T., De Felipe, C., Perez-Paya, E., Belmonte, C., Messeguer, A., Ferrer-Montiel, A., 2002. Attenuation of thermal nociception and hyperalgesia by VR1 blockers. Proc. Natl. Acad. Sci. U. S. A. 99, 2374–2379.

Gunthorpe, M.J., Benham, C.D., Randall, A., Davis, J.B., 2002. The diversity in the vanilloid (TRPV) receptor family of ion channels. Trends Pharmacol. Sci. 23, 183–191.

Huang, S.M., Bisogno, T., Trevisani, M., Al-Hayani, A., De Petrocellis, L., Fezza, F., Tognetto, M., Petros, T.J., Krey, J.F., Chu, C.J., Miller, J.D., Davies, S.N., Geppetti, P., Walker, J.M., Di Marzo, V., 2002. An endogenous capsaicin-like substance with high potency at recombinant and native vanilloid VR1 receptors. Proc. Natl. Acad. Sci. U. S. A. 99, 8400–8405.

Ishida, Y., Ugawa, S., Ueda, T., Murakami, S., Shimada, S., 2002. Vanilloid receptor subtype-1 (VR1) is specifically localized to taste papillae. Mol. Brain Res. 107, 17–22.

Kedei, N., Szabo, T., Lile, J.D., Treanor, J.J., Olah, Z., Iadarola, M.J., Blumberg, P.M., 2001. Analysis of the native quaternary structure of vanilloid receptor 1. J. Biol. Chem. 276, 28613–28619.

Kress, M., Zeilhofer, H.U., 1999. Capsaicin, protons and heat: new excitement about nociceptors. Trends Pharmacol. Sci. 20, 112–118.

Maggi, C.A., Patacchini, R., Santicioli, P., Giuliani, S., Geppetti, P., Meli, A., 1988. Protective action of ruthenium red toward capsaicin desensitization of sensory fibers. Neurosci. Lett. 88, 201–205.

Melchiorre, C., Cassinelli, A., Quaglia, W., 1987. Differential blockade of muscarinic receptor subtypes by polymethylene tetraamines. Novel class of selective antagonists of cardiac M-2 muscarinic receptors. J. Med. Chem. 30, 201–204.

Melchiorre, C., Quaglia, W., Picchio, M.T., Giardinà, D., Brasili, L., Angeli, P., 1989. Structure–activity relationships among methoctramine-related polymethylene tetraamines. Chain-length and substituent effects on M-2 muscarinic receptor blocking activity. J. Med. Chem. 32, 79–84.

Mellor, I.R., Usherwood, P.N.R., 2004. Targeting ionotropic receptors with polyamine-containing toxins. Toxicon 43, 493–508.

Mellor, I.R., Brier, T.J., Pluteanu, F., Strømgaard, K., Saghyan, A., Eldursi, N., Brierley, M.J., Andersen, K., Jaroszewski, J.W., Krogsgaard-Larsen, P., Usherwood, P.N.R., 2003. Modification of the philanthotoxin-343 polyamine moiety results in different structure–activity profiles at muscle nicotinic ACh, NMDA and AMPA receptors. Neuropharmacology 44, 70–80.

Minarini, A., Quaglia, W., Tumiatti, V., Melchiorre, C., 1989. An improved synthesis of *N*,*N*′ -bis[6-o-methoxyphenyl methyl hexylamino]-1,8-octanediamine (methoctramine). Chem. Ind. 19, 652–653.

Minarini, A., Budriesi, R., Chiarini, A., Melchiorre, C., Tumiatti, V., 1991. Further investigation on methoctramine-related tetraamines: effects of terminal N-substitution and of chain length separating the four nitrogens on M2 muscarinic receptor blocking activity. Farmaco 46, 1167–1178.

Mohapatra, D.P., Wang, S-Y., Wang, G.K., Nau, C., 2003. A tyrosine residue in TM6 of the vanilloid receptor TRPV1 involved in desensitization and calcium permeability of capsaicin-activated currents. Mol. Cell. Neurosci. 23, 314–324.

Montell, C., Birnbaumer, L., Flockerzi, V., Bindels, R.J., Bruford, E.A., Caterina, M.J., Clapham, D.E., Harteneck, C., Heller, S., Julius, D., Kojima, I., Mori, Y., Penner, R., Prawitt, D., Scharenberg, A.M., Schultz, G., Shimizu, N., Zhu, M.X., 2002. A unified nomenclature for the superfamily of TRP cation channels. Mol. Cell 9, 229–231.

Nagy, I., Rang, H.P., 1999. Similarities and differences between the responses of rat sensory neurons to noxious heat and capsaicin. J. Neurosci. 19, 10647–10655.

Oh, U., Hwang, S.W., Kim, D., 1996. Capsaicin activates a nonselective cation channel in cultured neonatal rat dorsal root ganglion neurons. J. Neurosci. 16, 1659–1667.

Planells-Cases, R., Aracil, A., Merino, J.M., Gallar, J., Perez-Paya, E., Belmonte, C., Gonzalez-Ros, J.M., Ferrer-Montiel, A.V., 2000. Arginine-rich peptides are blockers of VR-1 channels with analgesic activity. FEBS Lett. 481, 131–136.

Premkumar, L.S., Agarwal, S., Steffen, D., 2002. Single-channel properties of native and cloned rat vanilloid receptors. J. Physiol. 545, 107–117.

Quaglia, W., Giardinà, D., Marucci, G., Melchiorre, C., Minarini, A., Tumiatti, V., 1991. Structure–activity relationships among methoctramine-related polymethylene tetraamines: 3. Effect of the four nitrogens on M2 muscarinic blocking activity as revealed by symmetrical and unsymmetrical polyamines. Farmaco 46, 417–434.

Rosini, M., Budriesi, R., Bixel, M.G., Bolognesi, M.L., Chiarini, A., Hucho, F., Krogsgaard-Larsen, P., Mellor, I.R., Minarini, A., Tumiatti, V., Usherwood, P.N., Melchiorre, C., 1999. Design, synthesis, and biological evaluation of symmetrically and unsymmetrically substituted methoctramine-related polyamines as muscular nicotinic receptor non-competitive antagonists. J. Med. Chem. 42, 5212–5223.

Rosini, M., Bixel, M.G., Marucci, G., Budriesi, R., Krauss, M., Bolognesi, M.L., Minarini, A., Tumiatti, V., Hucho, F., Melchiorre, C., 2002. Structure–activity relationships of methoctramine-related polyamines as muscular nicotinic receptor noncompetitive antagonists: 2. Role of polymethylene chain lengths separating amine functions and of substituents on the terminal nitrogen atoms. J. Med. Chem. 45, 1860–1878.

Savidge, J.R., Ranasinghe, S.P., Rang, H.P., 2001. Comparison of intracellular calcium signals evoked by heat and capsaicin in cultured rat dorsal root ganglion neurons and in a cell line expressing the rat vanilloid receptor, VR1. Neuroscience 102, 177–184.

Seabrook, G.R., Sutton, K.G., Jarolimek, W., Hollingworth, G.J., Teague, S., Webb, J., Clark, N., Boyce, S., Kerby, J., Ali, Z., Chou, M., Middleton, R., Kaczorowski, G., Jones, A.B., 2002. Functional properties of the high-affinity TRPV1 (VR1) vanilloid receptor antagonist (4-hydroxy-5-iodo-3-methoxyphenylacetate ester) iodo-resiniferatoxin. J. Pharmacol. Exp. Ther. 303, 1052–1060.

Smart, D., Gunthorpe, M.J., Jerman, J.C., Nasir, S., Gray, J., Muir, A.I., Chambers, J.K., Randall, A.D., Davis, J.B., 2000. The endogenous lipid anandamide is a full agonist at the human vanilloid receptor (hVR1). Br. J. Pharmacol. 129, 227–230.

Smith, G.D., Gunthorpe, M.J., Kelsell, R.E., Hayes, P.D., Reilly, P., Facer, P., Wright, J.E., Jerman, J.C., Walhin, J.-P., Ooi, L., Egerton, J., Charles, K.J., Smart, D., Randall, A.D., Anand, P., Davis, J.B., 2002. TRPV3 is a temperature-sensitive vanilloid receptor-like protein. Nature 418, 186–190.

Strømgaard, K., Mellor, I., 2004. AMPA receptor ligands: synthetic and pharmacological studies of polyamines and polyamine toxins. Med. Res. Rev. 24, 589–620.

Szallasi, A., Blumberg, P.M., 1989. Resiniferatoxin, a phorbol-related diterpene, acts as an ultrapotent analog of capsaicin, the irritant constituent in red pepper. Neuroscience 30, 515–520.

Szallasi, A., Di Marzo, V., 2000. New perspectives on enigmatic vanilloid receptors. Trends Neurosci. 23, 491–497.

Trevisani, M., Smart, D., Gunthorpe, M.J., Tognetto, M., Barbieri, M., Campi, B., Amadesi, S., Gray, J., Jerman, J.C., Brough, S.J., Owen, D., Smith, G.D., Randall, A.D., Harrison, S., Bianchi, A., Davis, J.B., Geppetti, P., 2002. Ethanol elicits and potentiates nociceptor responses via the vanilloid receptor-1. Nat. Neurosci. 5, 546–551.

Urban, L., Dray, A., 1991. Capsazepine, a novel capsaicin antagonist, selectively antagonises the effects of capsaicin in the mouse spinal cord in vitro. Neurosci. Lett. 134, 9–11.

Wahl, P., Foged, C., Tullin, S., Thomsen, C., 2001. Iodo-resiniferatoxin, a new potent vanilloid receptor antagonist. Mol. Pharmacol. 59, 9–15.

Waldmann, R., Champigny, G., Bassilana, F., Heurteaux, C., Lazdunski, M., 1997. A proton-gated cation channel involved in acid-sensing. Nature 386, 173–177.

Welch, J.M., Simon, S.A., Reinhart, P.H., 2000. The activation mechanism of rat vanilloid receptor 1 by capsaicin involves the pore domain and differs from the activation by either acid or heat. Proc. Natl. Acad. Sci. U. S. A. 97, 13889–13894.

Zeilhofer, H.U., Kress, M., Swandulla, D., 1997. Fractional Ca^{2+} currents through capsaicin- and proton-activated ion channels in rat dorsal root ganglion neurones. J. Physiol. 503, 67–78.